Electronic Supplementary Material (ESI) for Dalton Transactions.
This journal is © The Royal Society of Chemistry 2019

Electronic Supplementary Information

A Biocompatible Redox MRI Probe Based on a Mn^{II}/Mn^{III} Porphyrin

Sara M. A. Pinto[a,b], Mário J. F. Calvete[a,b], Mariana E. Ghica,[a] Sérgio Soler[c], Iluminada Gallardo[c], Agnès Pallier[d], Mariana B. Laranjo,[b,e] Ana M.S. Cardoso,[f] M. Margarida C. A. Castro[b,e], Christopher M.A. Brett,[a] Mariette M. Pereira,[a,b]* Éva Tóth[d]* and Carlos F. G. C. Geraldes[b,c]*

[a]Department of Chemistry, Faculty of Science and Technology, University of Coimbra, Coimbra, Portugal
[b]Coimbra Chemistry Centre, CQC, University of Coimbra, Coimbra, Portugal
[c] Departament de Química, Universitat Autònoma de Barcelona, 08193 Bellaterra, Barcelona, Spain
[d]Centre de Biophysique Moléculaire, CNRS, UPR 4301, Université d'Orléans, Orléans, France
[e]Department of Life Sciences, Faculty of Science and Technology, University of Coimbra, Coimbra, Portugal
[f]Center of Neurosciences and Cell Biology, CNC, University of Coimbra, Coimbra, Portugal

*Correspondence to:
Carlos F. G. C. Geraldes, Department of Life Sciences, Faculty of Science and Technology, University of Coimbra, Calçada Martim de Freitas, 3000-393 Coimbra, Portugal; Tel. + 351239240730; email: geraldes@ci.uc.pt

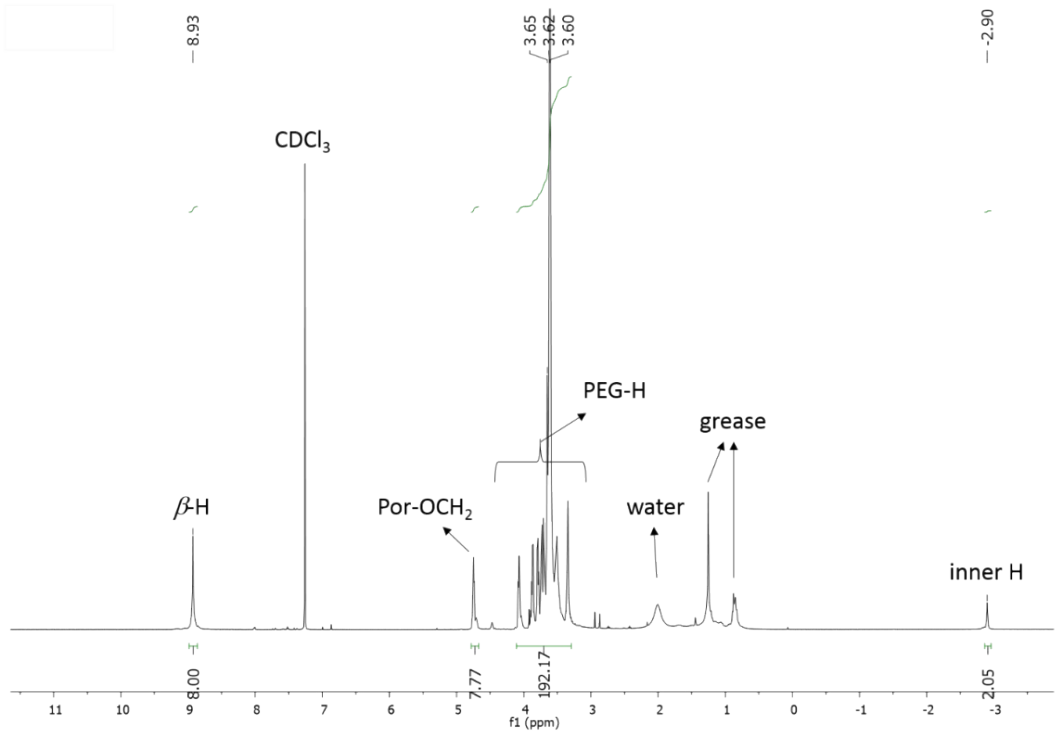

Fig. S1. ^{1}H NMR of Porphyrin **2**, acquired in $CDCl_3$.

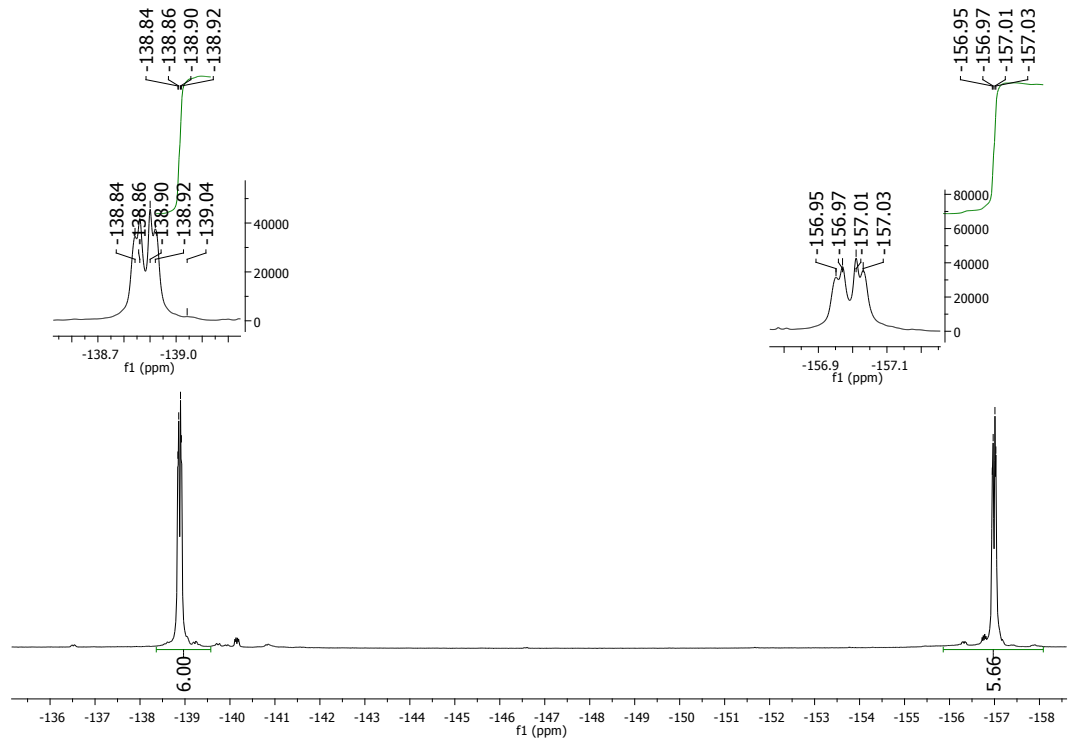

Fig. S2. ^{19}F NMR of Porphyrin **2**, acquired in $CDCl_3$.

RIAIDT
UNIDADE DE ESPECTROMETRIA DE MASAS E PROTEÓMICA
Edificio CACTUS * Campus Vida
15782 Santiago de Compostela (Spain)
Tel. 981 563 100. Ext. 16242 * Fax 981 528098
E-mail: sxemasas@usc.es
Web: http://www.ti.usc.es/riaidt/masas/masas.htm

ESPECTRO ESI-FIA-TOF

Analysis Info

Sample Name	SA2_2319_1-C,5_01_20317.d	Acquisition Date	4/25/2016 12:24:39 PM
Method	fia_pos_alto_400-3500_egf.m	Instrument	micrOTOF

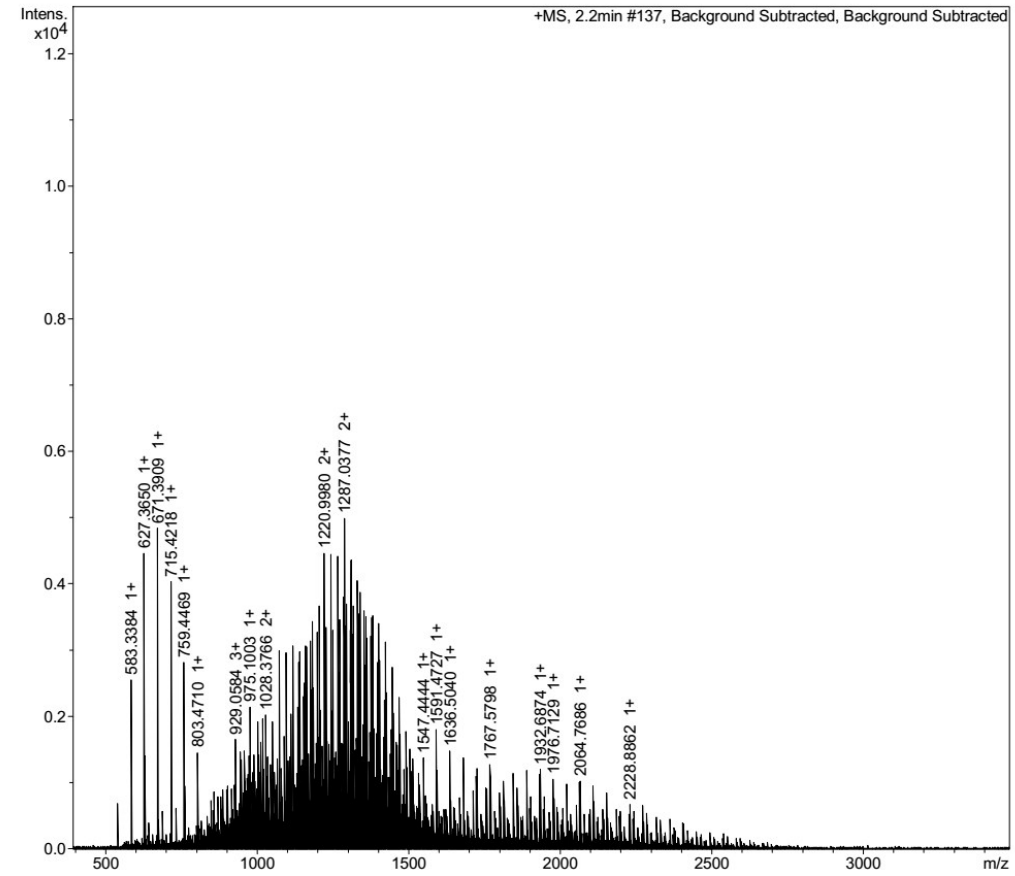

Bruker Compass DataAnalysis 4.0 printed: 4/26/2016 5:25:22 PM Page 1 of 11

Fig. S3. ESI-FIA-TOF mass spectrum of Porphyrin **2**.

RIAIDT
UNIDADE DE ESPECTROMETRIA DE MASAS E PROTEÓMICA
Edificio CACTUS * Campus Vida
15782 Santiago de Compostela (Spain)
Tel. 981 563 100. Ext. 16242 * Fax 981 528098
E-mail: sxemasas@usc.es
Web: http://www.ti.usc.es/riaidt/masas/masas.htm

ESPECTRO ESI-FIA-TOF

Analysis Info

Sample Name	SMP158PD_3072_1-A,1_01_20987.d	Acquisition Date	6/23/2016 12:33:11 PM
Method	fia_pos_alto_400-3500_egf.m	Instrument	micrOTOF

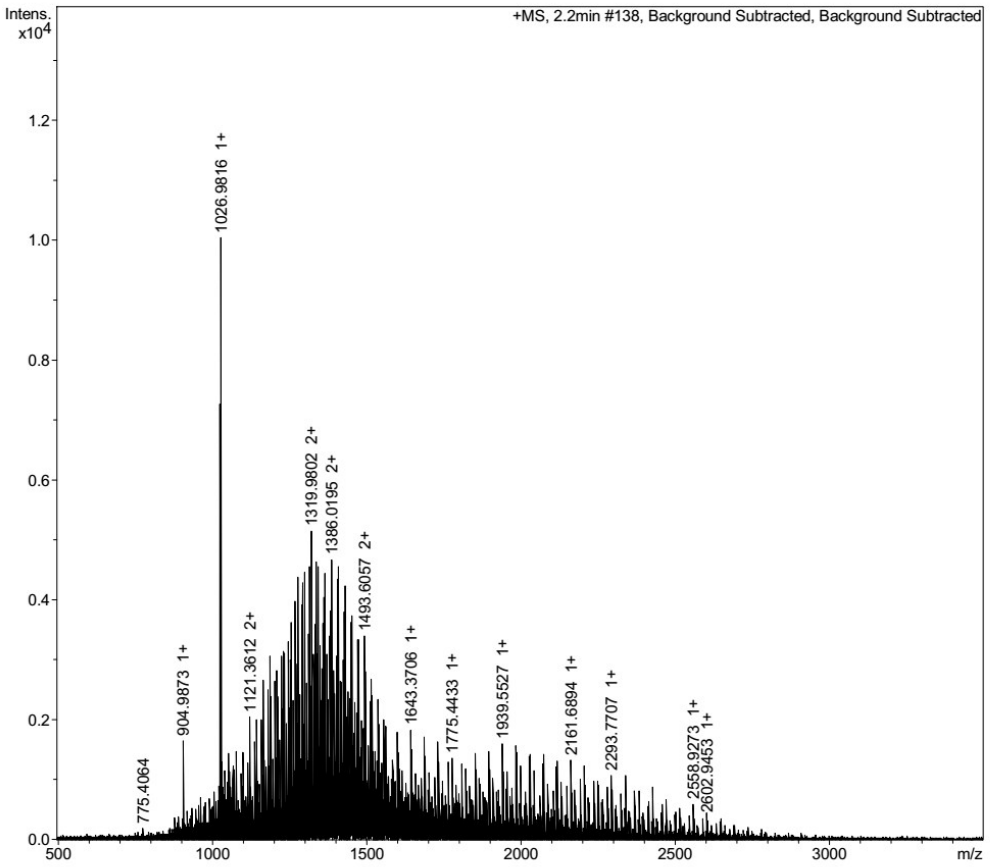

Bruker Compass DataAnalysis 4.0 printed: 6/23/2016 2:29:15 PM Page 1 of 11

Fig. S4. ESI-FIA-TOF mass spectrum of Mn^{III}-**3**.

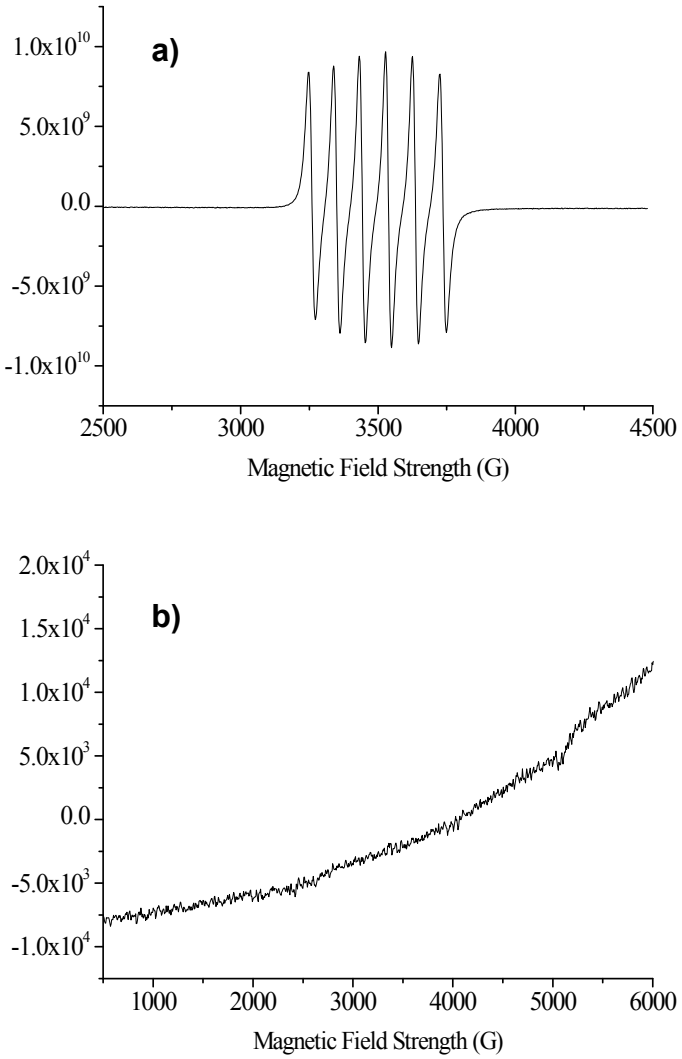

Fig. S5. EPR spectra at 25ºC of a) 1 mM $MnCl_2$ standard in PBS (pH 7.4) and b) 1 mM PBS (pH 7.4) solution of Mn^{III}–**3 (**amplification x 10^6)

a)

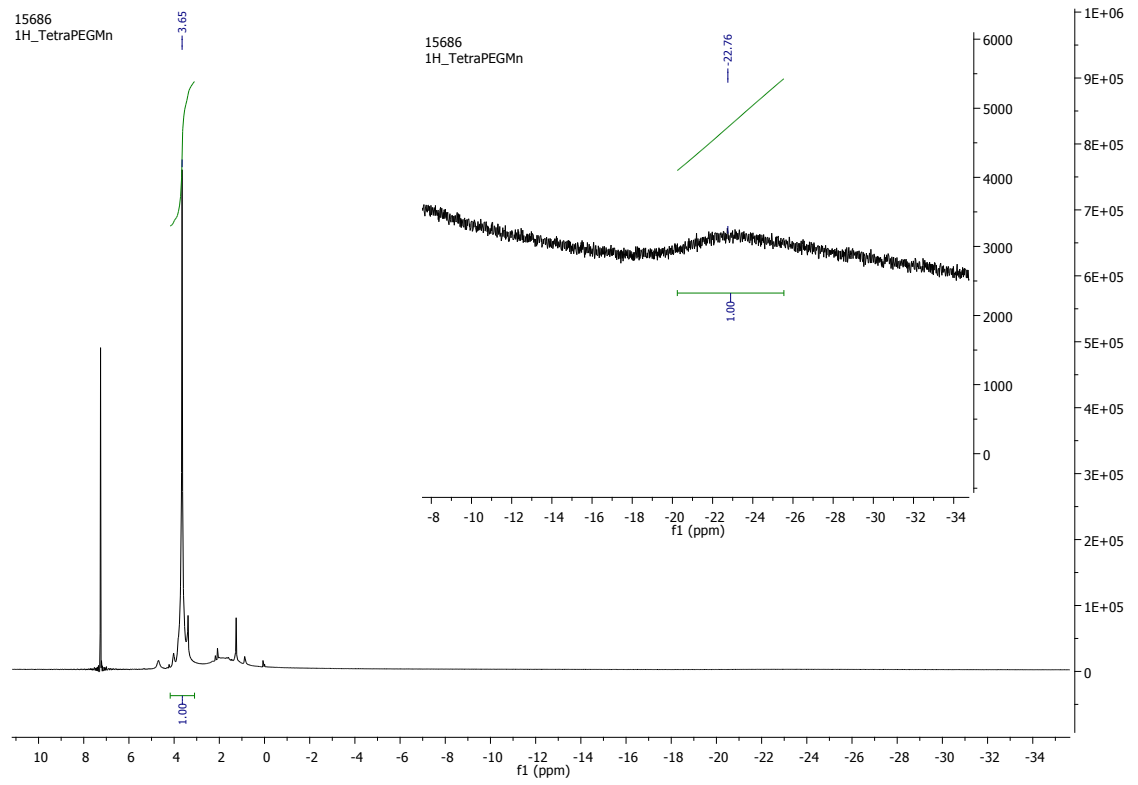
15686
1H_TetraPEGMn
3.65
1.00
f1 (ppm)
15686
1H_TetraPEGMn
22.76
1.00
f1 (ppm)

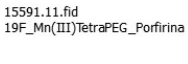
15591.11.fid
19F_Mn(III)TetraPEG_Porfirina


-127.26
-149.72
-152.53
-153.59
-156.64
-157.76

b)

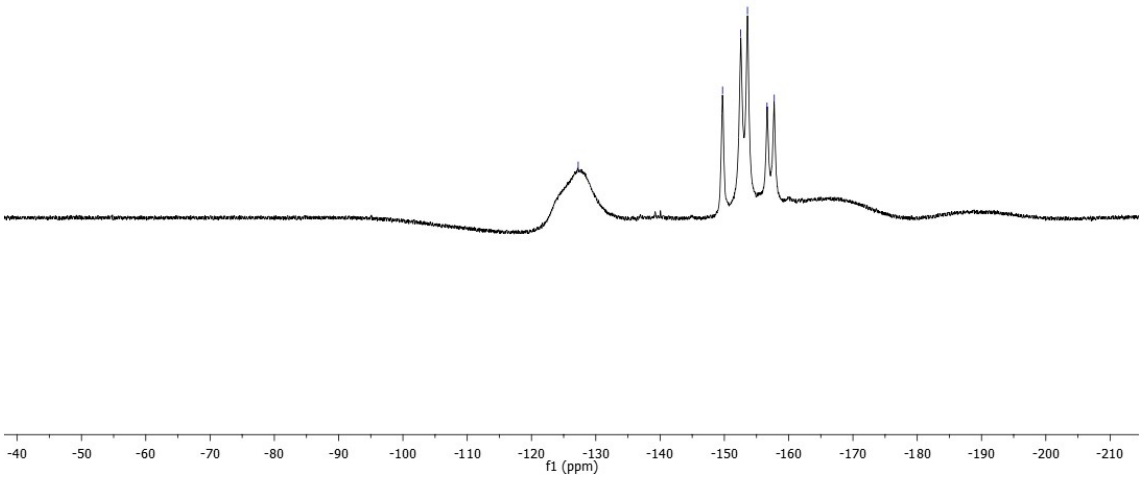
f1 (ppm)

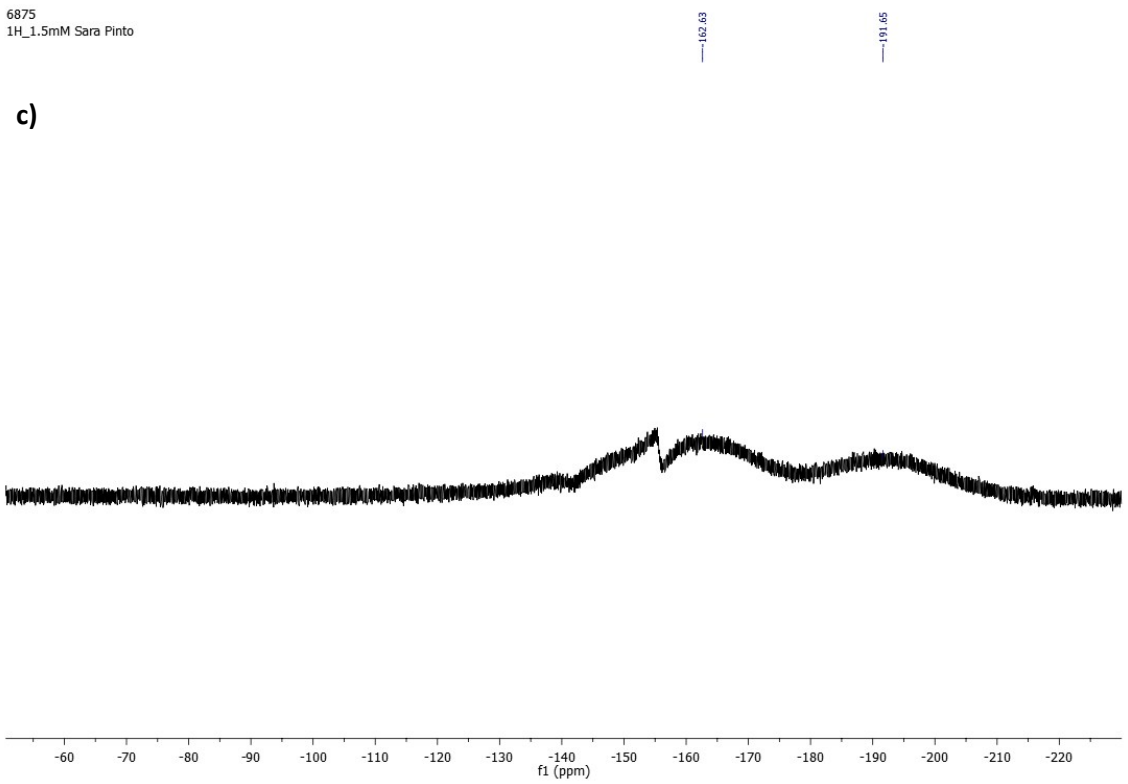

Fig. S6. a) ^{1}H and **b)** ^{19}F NMR spectra of 10 mM Mn^{III}**-3**; **c)** ^{19}F NMR after reduction to Mn^{II}**-3** in $CDCl_3$.

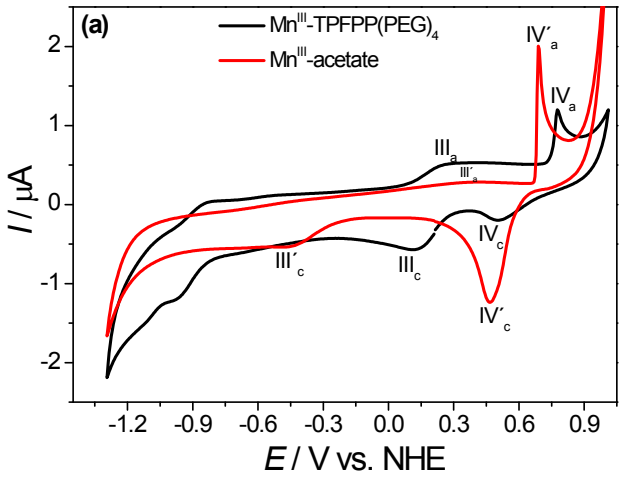
(a)
Mn^{III}-TPFPP(PEG)$_4$
Mn^{III}-acetate
IV´$_a$
IV$_a$
III$_a$
III´$_a$
IV$_c$
III´$_c$
III$_c$
IV´$_c$
I / µA
E / V vs. NHE

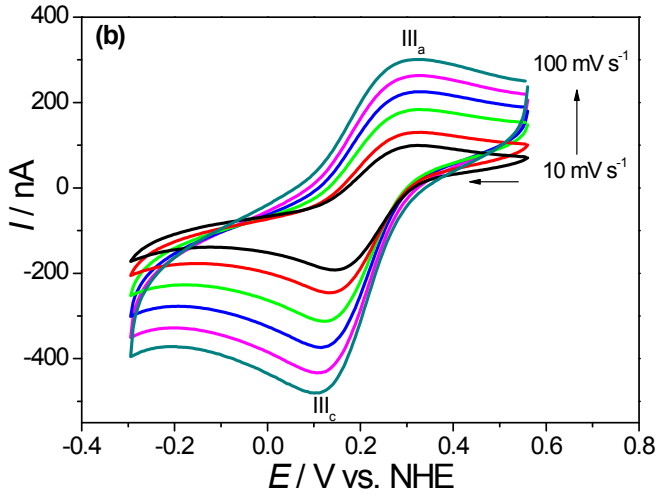
(b)
III$_a$
100 mV s^{-1}
10 mV s^{-1}
III$_c$
I / nA
E / V vs. NHE

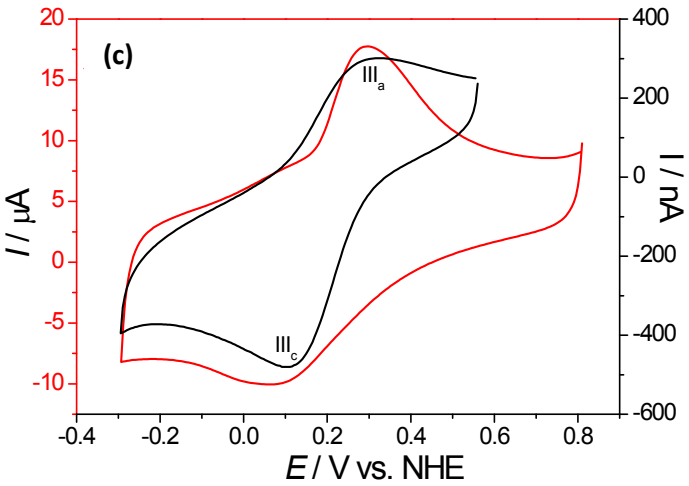
(c)
III$_a$
III$_c$
I / µA
I / nA
E / V vs. NHE

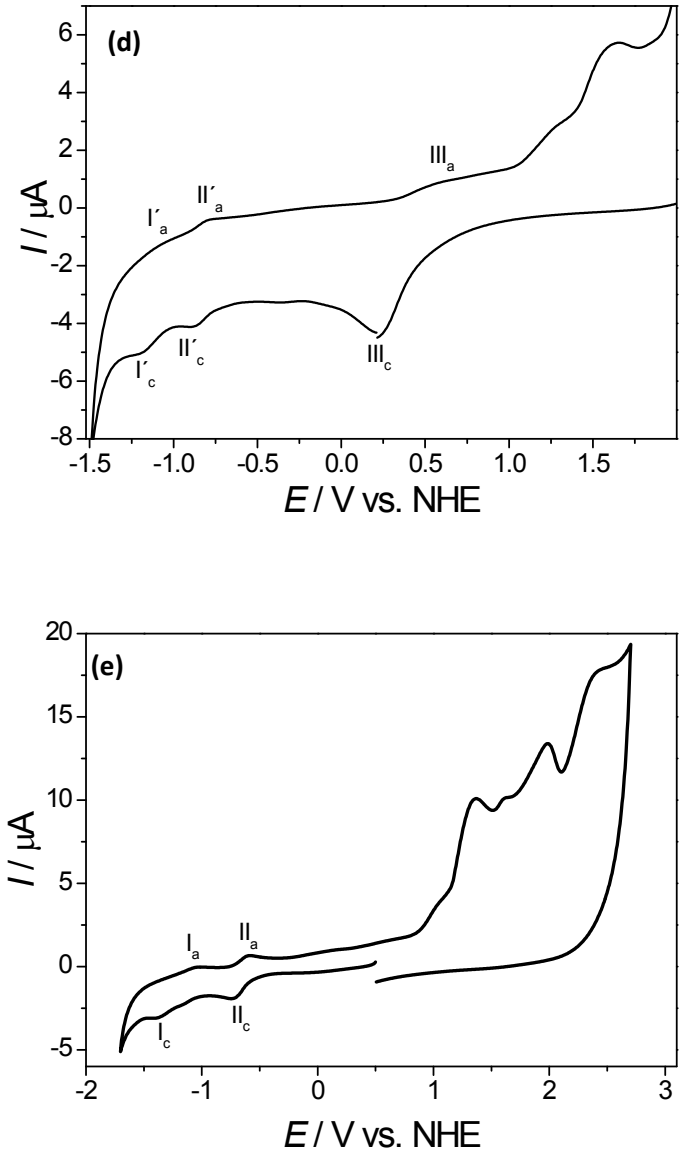

Fig. S7. Cyclic voltammetry at GCE in 0.1 M HEPES buffer pH 7.4 for (a) 2.2 mM of (black) Mn^{III}-TPPFP$(PEG)_4$ and (red) Mn^{III}-acetate, scan rate 100 mV s^{-1}; (b) 2.2 mM of Mn^{III}-TPFPP$(PEG)_4$ at scan rates 10 – 100 mV s^{-1} showing the Mn^{II}/Mn^{III} redox process; (c) of (red) 4.0 mM ascorbic acid and (black) 2.2 mM Mn^{III}-TPFPP$(PEG)_4$ in 0.1 M HEPES buffer pH 7.4; scan rate 100 mV s^{-1}; (d) 1.0 mM Mn^{III}-TPFPP$(PEG)_4$ in DCE + 0.6 M Bu_4NBF_4, scan rate 100 mV s-1 ; (e) 2.2 mM TPFPP$(PEG)_4$ in DCE + 0.6 M Bu_4NBF_4, scan rate 100 mV s^{-1}.

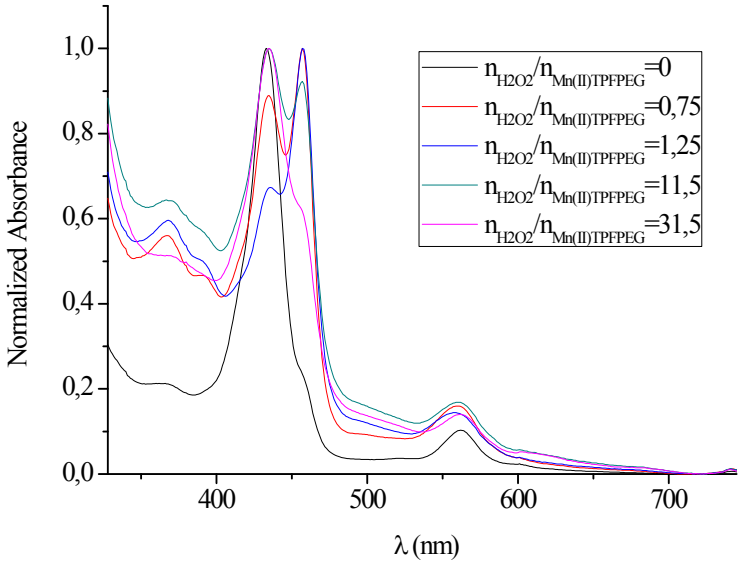

Fig. S8. UV-Vis spectra of the reoxidation of Mn^{II}-**3** with hydrogen peroxide recorded in PBS (25 ºC, pH = 7.4). Number of equivalents of ascorbic acid added: (black line) - 0; (red line) – 0.75; (blue line) – 1.25; (green line) – 11.5; (pink line) – 31.5.

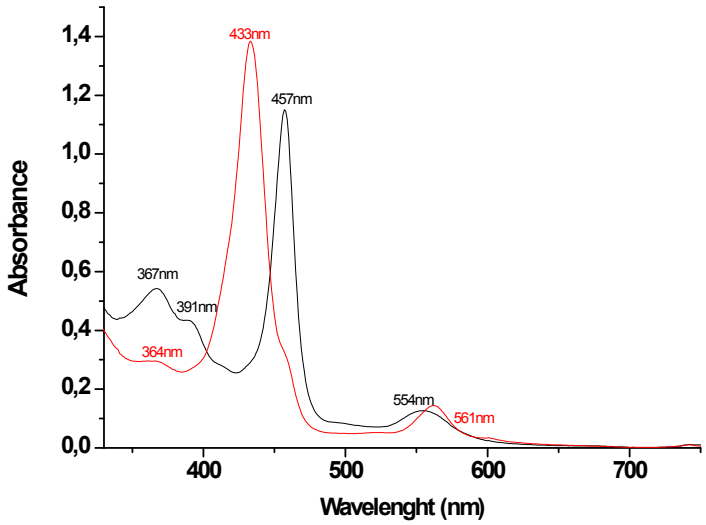

Fig. S9. UV-Vis spectrum of 0.041mM Mn^{III}-**3** in PBS (black line) and of Mn^{II}-**3** (red line) obtained 24 h after addition of 25.3 equivalents of ascorbic acid (25 ºC, pH = 7.4).

Kinetic Experiments for the reduction of Mn(III)-TPFPP(PEG)$_4$

In order to determine the empirical rate law for the reduction of Mn(III)-TPFPP(PEG)$_4$ by ascorbic acid, a series of kinetic experiments was conducted at 25°C (pH=7.4) under oxygen-free conditions using deaerated solutions under argon gas inside a sealed cuvette. The UV-Vis spectrum of Mn(III)-TPFPP(PEG)$_4$ has a strong absorbance band at 457 nm (ε=1.01×10^{4}M^{-1}s^{-1}). As the reduction occurs, this band disappears and a new band at 434 nm appears, typical of Mn(II)-TPFPP(PEG)$_4$. This feature was used to follow the reduction of Mn(III)-TPFPP(PEG)$_4$ over time.

Initial reaction rates were measured by maintaining the concentration of Mn(III)-TPFPP(PEG)$_4$ (8 μM) and using three different initial concentrations of ascorbic acid (390 μM, 191 μM, 91 μM). Additionally, other experiments were performed by maintaining the concentration of ascorbic acid (9.7×10^3 μM) and using three different initial concentrations of Mn(III)-TPFPP(PEG)$_4$ (230 μM, 150 μM, 95 μM). In both experiments a large excess of ascorbic acid was used and we concluded that the reduction reaction was pseudo first-order with respect to Mn(III)-TPFPP(PEG)$_4$ as expressed in equation S1.

$$ln[\text{Mn(III)-TPFPP(PEG)}_4]_t = ln[\text{Mn(III)-TPFPP(PEG)}_4]_0 - k_{obs}\, t \quad \text{(equation S1)}$$

where the observed rate constant (k_{obs}) is the product of the actual rate constant (k) and [ascorbic acid]$_0$, t is the time, and the subscripts 't' and '0' refer to the concentration at time 't' and initial concentration, respectively.

Figure S10 and S11 show the two sets of kinetic experiments in which we have plotted the ln[Mn(III)-TPFPP(PEG)$_4$]$_t$ as a function of time. The slope of each line is equal to $-k_{obs} = -k$ [ascorbic acid]$_0$ and the intercept is ln[Mn(III)-TPFPP(PEG)$_4$]$_0$. In Figure S10 the intercept is the same and the negative slope increases with [ascorbic acid]$_0$, while in Figure S11 the slopes are the same and the intercept increases with ln[Mn(III)-TPFPP(PEG)$_4$]$_0$. The analysis of the experiments showed that the reaction was first-order relatively to both ascorbic acid and Mn(III)-TPFPP(PEG)$_4$ concentrations, with an overall second-order rate constant $k = k_2 = 46.1 \pm 5.6$ M^{-1} s^{-1}.

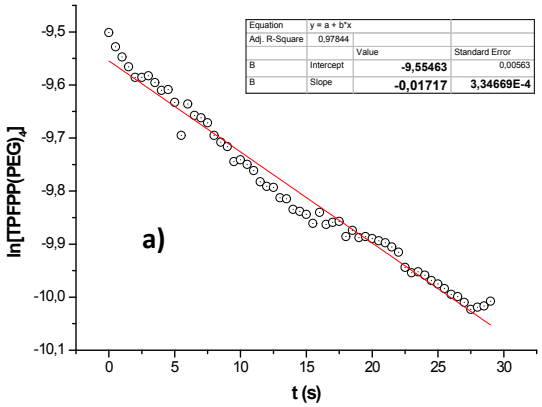

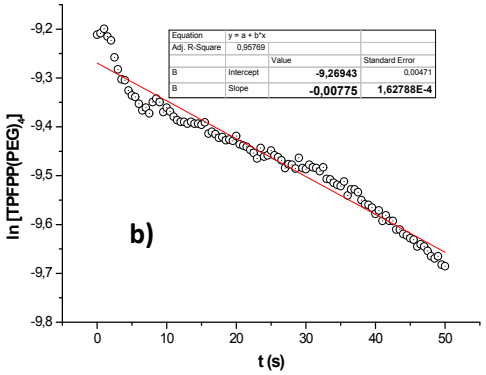

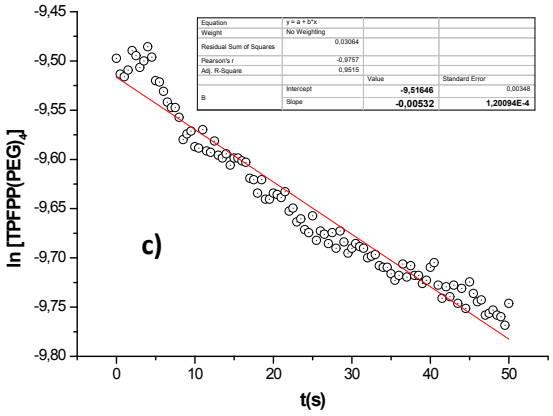

Fig. S10. Log plots where the concentration of Mn^{III}-TPFPP(PEG)$_4$ was constant at 8 μM and the concentration of ascorbic acid was varied: a) [ascorbic acid] =390 μM; b) 1901 μM; c) 91μM (following the disappearance of the Soret band at 457nm with time due to the reduction).

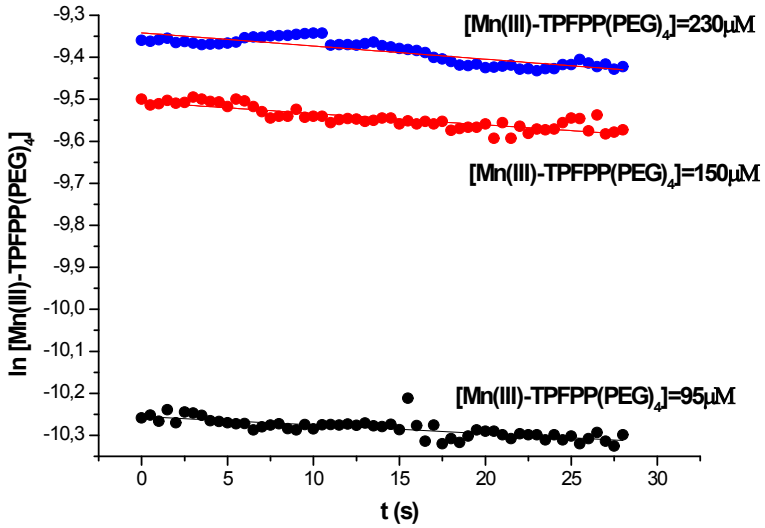

Fig. S11. Log plots where the concentration of ascorbic acid was constant at 9.7×10^3 μM and the concentration of Mn^{III}-TPFPP(PEG)$_4$ was varied (following the disappearance of the Soret band at 457nm with time due to the reduction).

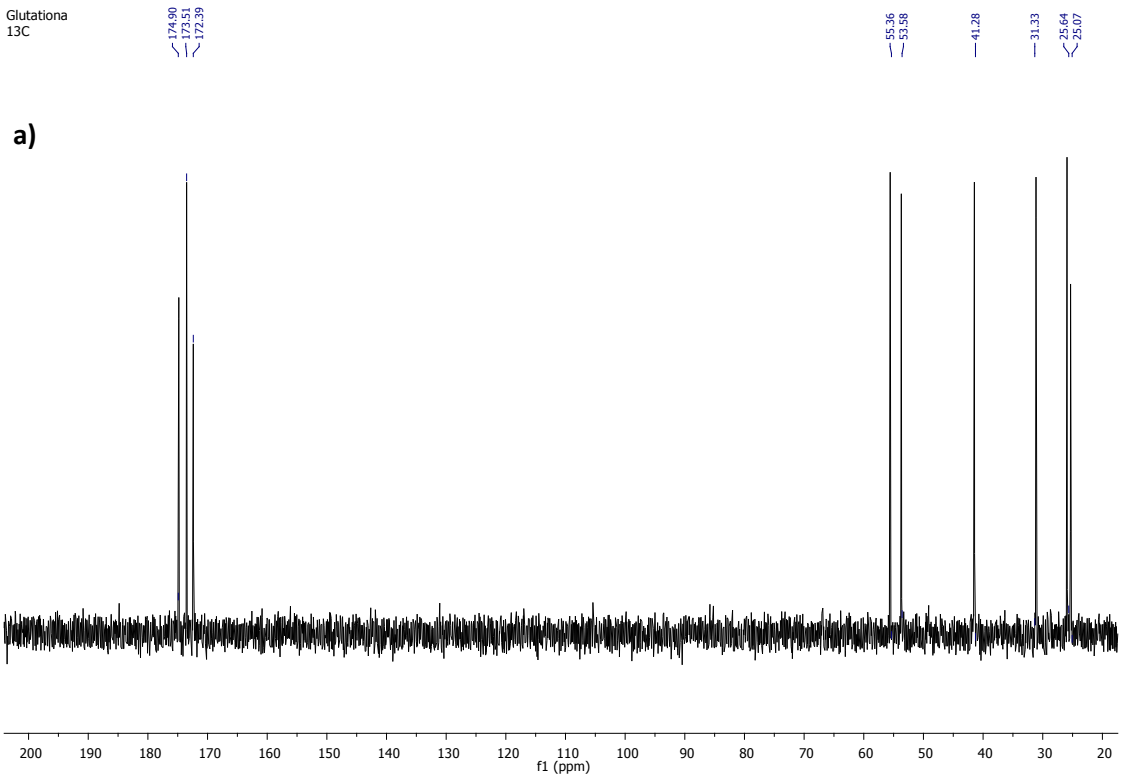
Glutationa
13C
174.90
173.51
172.39
55.36
53.58
41.28
31.33
25.64
25.07
a)
200 190 180 170 160 150 140 130 120 110 100 90 80 70 60 50 40 30 20
f1 (ppm)

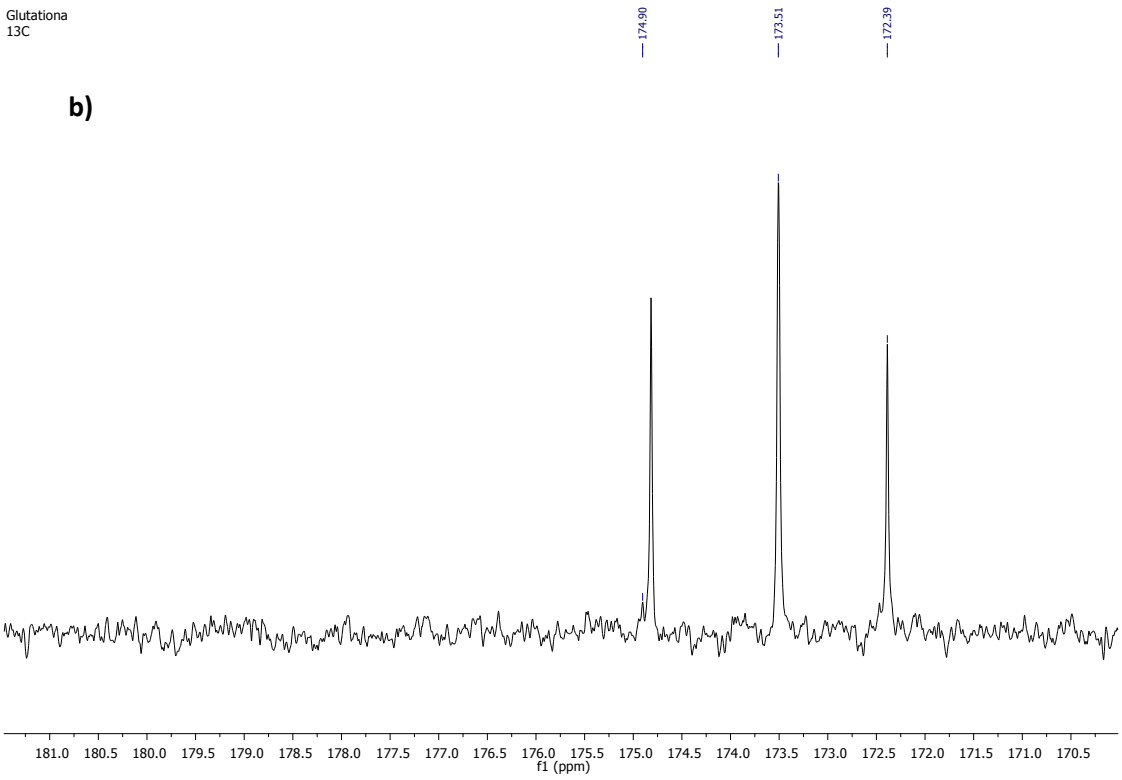
Glutationa
13C
174.90
173.51
172.39
b)
181.0 180.5 180.0 179.5 179.0 178.5 178.0 177.5 177.0 176.5 176.0 175.5 175.0 174.5 174.0 173.5 173.0 172.5 172.0 171.5 171.0 170.5
f1 (ppm)

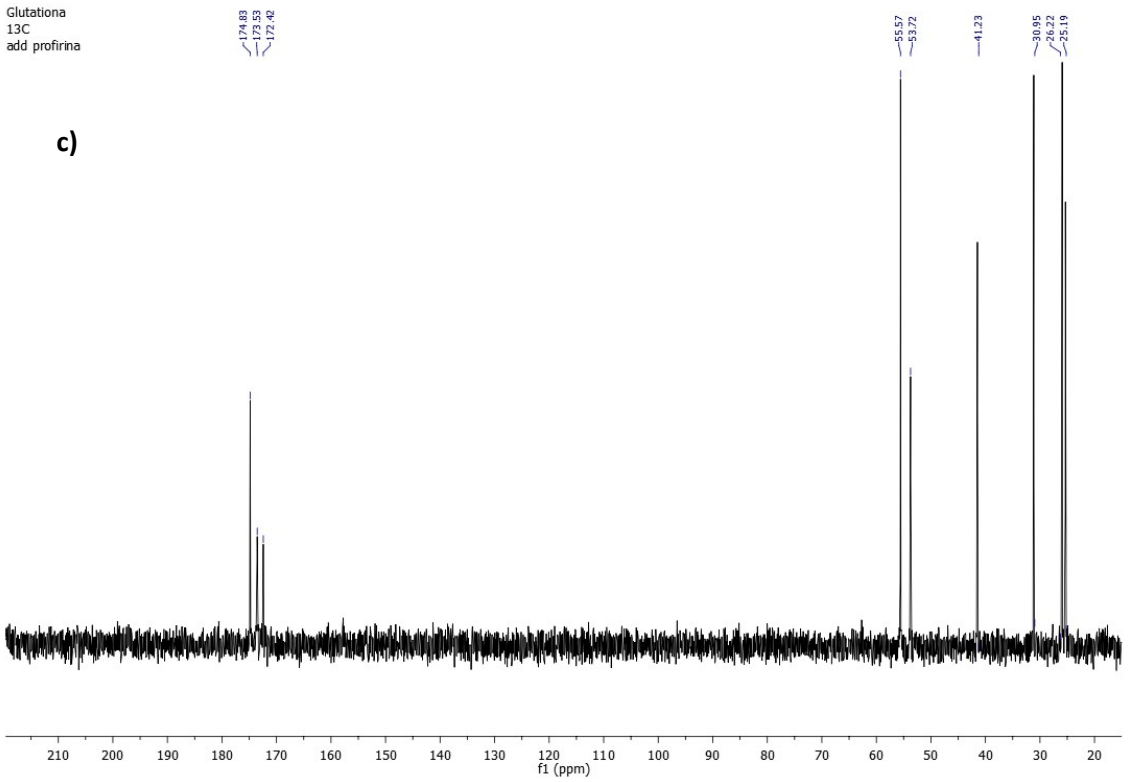

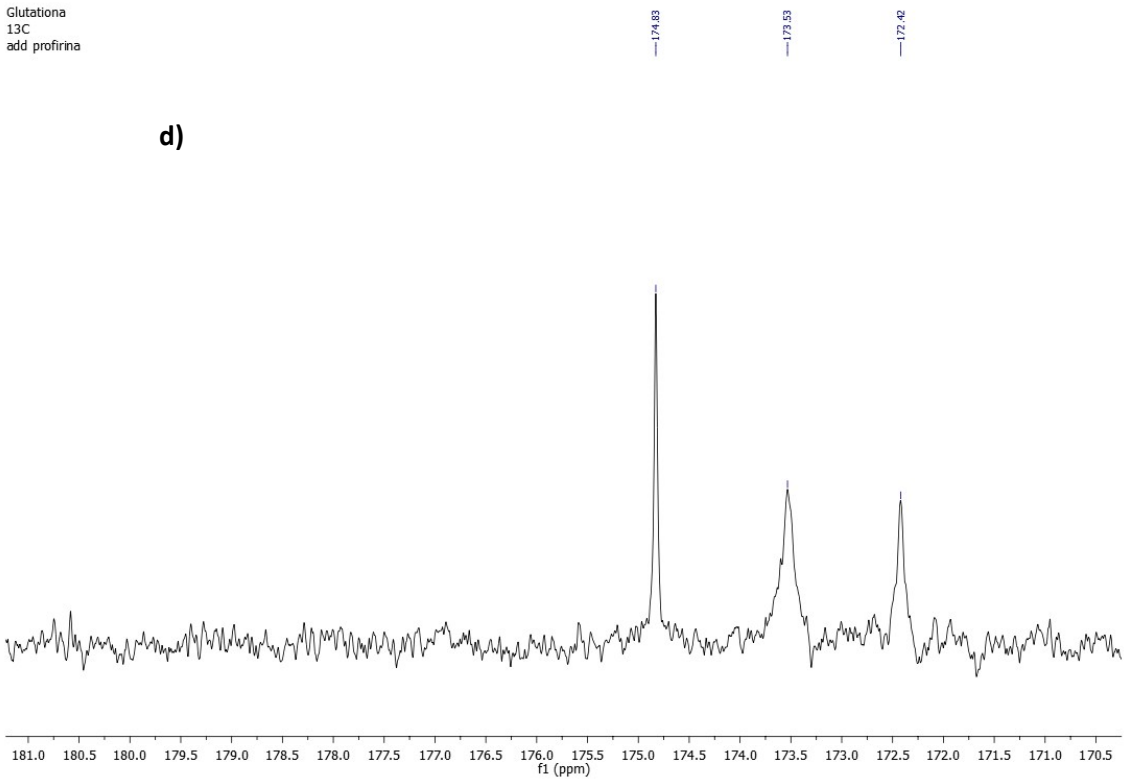

Fig. S12. ^{13}C NMR of **a)** and **b)** gluthatione **c)** and **d)** glutathione with 0.1 equiv of Mn^{III}-**3** in D_2O.

Table S1. Reduction potentials (vs NHE) of **3,** Zn^{II}-(**3**) and Mn^{III}-(**3**) in DCE + 0.6 M Bu_4NBF_4 at glassy carbon working electrode. These data are compared with literature values for some perfluorinated tetraphenylporphyrins in non-aqueous solvents.

	Side chains	Porphyrin		Metal	Porphyrin		Side chains		
Porphyrin	E′ox(3)	E′ox(2)	E′ox(1)	E′Mox/red	E′red(1)	E′red(2)	E′red(3)	E′red(4)	Ref.
3	*	*	*	-	-0.452	-1.00	*	-	**tw**
Zn^{II}-(3)	+2.80	+1.82	+1.57	-	-0.72	-1.10	-0.94	-1.31	**tw**
Zn^{II}-TFPP[a]	-	+1.80	+1.59	-	-0.73	-1.15	-	-	1
Zn^{II}-TPFPPy[b]	-	+1.32	+1.20	-	-1.19	-1.55	-	-	2
Mn^{III}-(3)	*	*	*	+0.335	-0.828	-1.131	*	-	**tw**
Mn^{III}-TFPP[a]	-	+1.8 (2e)	-	+0.05	-1.04	-1.47	-	-	3
Mn^{III} -TPFPPy[b]	-	+1.42	+1.22	-0.12	-1.24	-1.65	-		2
Mn^{III} – $(PFP)_3(DMP)$[c]	-	+1.8 (2e)	-	+0.558	-	-0.999 (2e)	-	-	4
Mn^{III} – t-$(PFP)_2(DMP)$[c]	-	+1.8 (2e)	-	+0.440	-0.48	-0.926	-	-	4
Mn^{III} – c-$(PFP)_2(DMP)$[c]	-	+1.8 (2e)	-	+0.413	-0.35	-0.882	-	-	4

[a]TFPP = tetrakis(pentafluorophenyl)porphyrin: [b]TPFPPy = tetrakis(p-[3-(pyrrol-1-yl)propyloxy] tetrafluorophenyl)porphyrin; c PFP =pentafluorophenyl, DMP = 3,4-dimethoxyphenyl; * Not measured; tw = this work.; 1. Hodge, J.A.; Hill, M.G.; Gray, H.B. Inorg. Chem., 1995, 34, 809; 2. de Medeiros, M. A. C.; Gorgy, K.; Deronzier, A.; Cosnier, S. *Mat. Sci. Eng. C*, **2008**, *28*, 731 ; 3. Friedermann, G.R.; Halma, M.; Castro, K. A. D. F., Benedito, F.L.; Doro, F. G.; Drechsel, S. M.; Mangrich, A. S.; Assis, M. D.; Nakagaki, S. *Applied Catalysis A: General* **2006**, *308*, 172 ; 4. Antonangelo, A. R.; Westrup, K. C. M. ; Burt, L. A. ; Grazia Bezzu, C. ; Malewschik, T.; Machado, G. S.; Nunes, F. S.; McKeown, N. B.; Nakagaki, S. *RSC Adv*., **2017**, *7*, 50610.

Equations used for treatment of the relaxometric data

The proton relaxivities (normalized to 1 mM Mn^{2+} concentration) originate from inner- and outer-sphere contributions (Equation (S1)):

$$r_1 = r_{1is} + r_{1os} \tag{S1}$$

The inner-sphere term is given by Equation (S2), where q is the number of inner-sphere water molecules.

$$r_{1is} = \frac{1}{1000} \times \frac{q}{55.55} \times \frac{1}{T_{1m}^{H} + \tau_m} \tag{S2}$$

In the longitudinal relaxation rate of inner sphere water protons, $1/T_{1m}^{H}$, the dipolar contribution dominates (Equation (S3)):

$$\frac{1}{T_{1m}^{H}} \cong \frac{1}{T_1^{DD}} = \frac{2}{15}\left(\frac{\mu_0}{4\pi}\right)^2 \frac{\hbar^2 \gamma_S^2 \gamma_I^2}{r_{MnH}^6} S(S+1)\left[\frac{3\tau_{d1H}}{1+\omega_I^2\tau_{d1H}^2} + \frac{7\tau_{d2H}}{1+\omega_S^2\tau_{d2H}^2}\right] \tag{S3}$$

Here r_{MnH} is the effective distance between the Mn^{2+} electron spin and the water protons, ω_I is the proton resonance frequency, τ_{diH} is given by Eq. 4, where τ_{RH} is the rotational correlation time of the Mn^{2+}–H_{water} vector:

$$\frac{1}{\tau_{diH}} = \frac{1}{\tau_m} + \frac{1}{\tau_{RH}} + \frac{1}{T_{ie}} \qquad i = 1, 2; \tag{S4}$$

$$\tau_{RH} = \tau_{RH}^{298} \exp\left\{\frac{E_R}{R}\left(\frac{1}{T} - \frac{1}{298.15}\right)\right\} \tag{S5}$$

The electronic relaxation is mainly governed by modulation of the transient zero-field splitting, and for the electron spin relaxation rates, $1/T_{1e}$ and $1/T_{2e}$, McMachlan has developed Equations (S6)–(S8)[1] which were used in the fit of the NMRD data:

$$\left(\frac{1}{T_{1e}}\right) = \frac{32}{25}\Delta^2\left(\frac{\tau_v}{1+\omega_S^2\tau_v^2} + \frac{4\tau_v}{1+4\omega_S^2\tau_v^2}\right) \tag{S6}$$

$$\left(\frac{1}{T_{2e}}\right) = \frac{32}{50}\Delta^2\left[3\tau_v + \frac{5\tau_v}{1+\omega_S^2\tau_v^2} + \frac{2\tau_v}{1+4\omega_S^2\tau_v^2}\right] \tag{S7}$$

$$\tau_v = \tau_v^{298} \exp\left\{\frac{E_v}{R}\left(\frac{1}{T} - \frac{1}{298.15}\right)\right\} \tag{S8}$$

where Δ^2 is the trace of the square of the transient zero-field-splitting (ZFS) tensor, τ_v is the correlation time for the modulation of the ZFS with the activation energy E_v, and ω_s is the Larmor frequency of the electron spin.

The outer-sphere contribution to the overall relaxivity is described by Equation (S9), where N_A is the Avogadro constant, and J_{os} is a spectral density function (Equation (S10)).

$$r_{1os} = \frac{32N_A\pi}{405}\left(\frac{\mu_0}{4\pi}\right)^2 \frac{\mathrm{h}^2\gamma_S^2\gamma_I^2}{a_{MnH}D_{MnH}} S(S+1)\left[3J_{os}(\omega_I, T_{1e}) + 7J_{os}(\omega_S, T_{2e})\right] \quad \text{(S9)}$$

$$J_{os}(\omega, T_{je}) = \mathrm{Re}\left[\frac{1 + \frac{1}{4}\left(i\omega\tau_{MnH} + \frac{\tau_{MnH}}{T_{je}}\right)^{1/2}}{1 + \left(i\omega\tau_{MnH} + \frac{\tau_{MnH}}{T_{je}}\right)^{1/2} + \frac{4}{9}\left(i\omega\tau_{MnH} + \frac{\tau_{MnH}}{T_{je}}\right) + \frac{1}{9}\left(i\omega\tau_{MnH} + \frac{\tau_{MnH}}{T_{je}}\right)^{3/2}}\right]$$

$j = 1, 2$ (S10)

The diffusion coefficient for the diffusion of a water proton away from a Mn^{2+} complex, D_{MnH}, obeys the exponential temperature dependence described by Equation (S11), with activation energy E_{MnH}:

$$D_{MnH} = D_{MnH}^{298} \exp\left\{\frac{E_{MnH}}{R}\left(\frac{1}{298.15} - \frac{1}{T}\right)\right\} \quad \text{(S11)}$$

[1] McLachlan, A. D. *Proc. R. Soc. London, Ser. A.* **1964**, *280*, 271–288.